J Neuropathol Exp Neurol
Vol. 81, No. 11, November 2022, pp. 885–899
doi: 10.1093/jnen/nlac073

OXFORD

ORIGINAL ARTICLE

Developmentally Arrested Basket/Stellate Cells in Postnatal Human Brain as Potential Tumor Cells of Origin for Cerebellar Hemangioblastoma in von Hippel-Lindau Patients

Sharon Baughman Shively, MD, PhD, Nancy A. Edwards, Tobey J. MacDonald, MD, Kory R. Johnson, PhD, Natalia M. Diaz-Rodriguez, MD, Marsha J. Merrill, PhD, and Alexander O. Vortmeyer, MD, PhD

Abstract

von Hippel-Lindau (VHL) disease is an autosomal dominant hereditary cancer disorder caused by a germline mutation in the *VHL* tumor suppressor gene. Loss of the wild-type allele results in VHL deficiency and the potential formation of cerebellar hemangioblastomas, which resemble embryonic hemangioblast proliferation and differentiation processes. Multiple, microscopic, VHL-deficient precursors, termed developmentally arrested structural elements (DASEs), consistently involve the cerebellar molecular layer in VHL patients, indicating the tumor site of origin. Unlike hemangioblastomas, however, cerebellar DASEs do not express brachyury, a mesodermal marker for hemangioblasts. In this study, neuronal progenitors occupying the molecular layer were investigated as tumor cells of origin. By immunohistochemistry, cerebellar DASEs and hemangioblastomas lacked immunoreactivity with antibody ZIC1 (Zic family member 1), a granule cell progenitor marker with concordance from oligonucleotide RNA expression array analyses. Rather, cerebellar DASEs and hemangioblastomas were immunoreactive with antibody PAX2 (paired box 2), a marker of basket/stellate cell progenitors. VHL cerebellar cortices also revealed PAX2-positive cells in Purkinje and molecular layers, resembling the histological and molecular development of basket/stellate cells in postnatal non-VHL mouse and human cerebella. These data suggest that *VHL* deficiency can result in the developmental arrest of basket/stellate cells in the human cerebellum and that these PAX2-positive, initiated cells await another insult or signal to form DASEs and eventually, tumors.

Key Words: Developmentally arrested basket/stellate cells, Hemangioblastoma, Paired box 2 (PAX2), Tumor suppressor syndrome, VHL human cerebellum tumor cell of origin, von Hippel-Lindau (VHL) disease.

INTRODUCTION

von Hippel-Lindau (VHL) disease is an autosomal dominant hereditary cancer disorder, affecting approximately 1 in 35 000 persons (1). These patients inherit one dysfunctional copy of the *VHL* tumor suppressor gene (3p25-26), rendering them susceptible to developing particular tumors in selective organs secondary to loss of the functional, wild-type *VHL* allele (1–3). Tumors associated with VHL include hemangioblastoma, renal clear cell carcinoma, pheochromocytoma, microcystic adenoma and neuroendocrine tumor of the pancreas, epididymal cystadenoma, and endolymphatic sac tumor. The classic tumor is the hemangioblastoma of the nervous system, which forms primarily in the cerebellum, brainstem, spinal cord, and retina (4). Hemangioblastoma is a benign tumor composed of stromal cells and abundant capillaries but it can cause significant morbidity and mortality in VHL patients.

Lindau, after whom the disease is partially named, noted multiple neoplasms arising in the cerebellum, brainstem, spinal cord, and retina, and the apparent embryological phenotype of the tumor cells; he concluded that the neoplasm must be a vascular congenital anlage (5). A contemporary of Lindau, Sabin elucidated the origin of the vascular system (6, 7).

From the Surgical Neurology Branch, National Institute of Neurological Disorders and Stroke, National Institutes of Health, Bethesda, Maryland, USA (SBS, NAE, NMD-R, MJM, AOV); Department of Molecular Medicine, Institute for Biomedical Sciences, The George Washington University, Washington, District of Columbia, USA (SBS); Department of Pediatrics, Emory University, Atlanta, Georgia, USA (TJM); Bioinformatics Section, National Institute of Neurological Disorders and Stroke, National Institutes of Health, Bethesda, Maryland, USA (KRJ).

Send correspondence to: Alexander O. Vortmeyer, MD, PhD, Division of Neuropathology, Department of Pathology and Laboratory Medicine, Indiana University-Purdue University Indianapolis, 350 W. 11th Street, Suite 4034, Indianapolis, IN 46202, USA; E-mail: avortmey@iu.edu.

Present address: Natalia M. Diaz-Rodriguez, Department of Anesthesiology and Critical Care Medicine, Johns Hopkins University, Baltimore, Maryland, USA.

Present address: Alexander O. Vortmeyer, Department of Pathology, Indiana University-Purdue University Indianapolis, Indianapolis, Indiana, USA.

Marsha J. Merrill and Alexander O. Vortmeyer contributed equally to this work.

This study was supported by the Intramural Research Program of the National Institute of Neurological Disorders and Stroke (NINDS) and the Institute for Biomedical Sciences at the George Washington University.

The authors have no duality or conflicts of interest to declare.

Supplementary Data can be found at academic.oup.com/jnen.

She observed in chick embryo proper the developmental process of hemangioblast formation and differentiation from mesoderm. She noted that the central cells liquefy to form blood plasma and the bordering hemangioblasts then form the endothelial lining. Finally, the hemangioblasts and endothelial cells create blood islands that differentiate into red blood cells with hemoglobin. After studying Sabin's research, Cushing and Bailey (8) proposed that the neoplasm described by Lindau is composed of the same elements that enter into the development of the primordial blood channels. They, therefore, designated the neoplastic counterpart as "hemangioblastoma." The ensuing decades resulted in multiple attempts to find the VHL nervous system tumor cell of origin (9). The general theme of these studies is the identification of structures and molecules in tumor, then extrapolation of the discovery to propose the cell of origin, including hemangioblastic, mesenchymal, endothelial, neuroectodermal, neuroendocrine, and astrocytic cells.

Loss of heterozygosity (LOH) experiments demonstrate that stromal cells of hemangioblastomas lack the wild-type *VHL* allele (10). As a consequence, stromal cells constitutively express hypoxia-inducible factor 1 alpha subunit (HIF1α) and hypoxia-inducible factor 2 alpha subunit (HIF2α) (endothelial PAS domain protein 1), plus the HIF transcriptional targets vascular endothelial growth factor (VEGF) and carbonic anhydrase IX (CAIX), indicating biochemical sequelae of lost functional VHL protein (pVHL) (11–14). Further microscopic structural, immunohistochemical, and LOH studies demonstrate that VHL-deficient cells of hemangioblastomas engage in a hemangioblast maturation process. Hemangioblastomas can contain structures resembling normal embryonic blood islands and foci of extramedullary hematopoiesis. The nascent red blood cells comprising the extramedullary hematopoiesis express fetal hemoglobin and show LOH of the wild-type *VHL* gene (15). In addition, stromal cells express brachyury and T-cell acute lymphocytic leukemia 1 (TAL1, SCL), 2 transcription factors transiently expressed in hemangioblasts during embryogenesis (16). Hence, both hemangioblasts and hemangioblastomas share the expression of specific embryonic markers and the capability of erythrogenic and vasculogenic differentiation (6, 7, 15–20).

VHL patients can develop multiple nervous system hemangioblastomas over their lifetimes (21). As such, VHL patients uniquely harbor multiple, clinically undetectable precursors in various stages of progression to tumors. In VHL patient autopsies, multiple spinal nerve roots (primarily dorsal nerve roots) contain a uniform phenotype of microscopic abnormal foci composed of loosely scattered, poorly differentiated cells with small nuclei and little cytoplasm that are entwined by abundant capillaries and structurally resemble mesenchymal (i.e. capillary, reticular, juvenile) hemangioblastomas (22–24). These poorly differentiated cells demonstrate loss of the wild-type *VHL* gene and express HIF2α, VEGF, and CAIX. Unlike hemangioblastomas, however, they do not express HIF1α. The authors newly termed these microscopic, neoplastic foci of immature cells as "developmentally arrested structural elements (DASEs)," distinct from "hamartoma," which are described as benign, focal, disorganized overgrowth of mature cells indigenous to the affected organ, and frank "tumor" (25).

Three-dimensional reconstructions of spinal nerve root DASEs and study of tumors from the spinal cord, cerebellum, and brainstem of VHL surgical and autopsy patients reveal a distinct structural and molecular progression pattern for hemangioblastomas. In the spinal cord, DASEs solely involve nerve roots, whereas tumors involve nerve roots with extensions into the cord, thus identifying the nerve root as a consistent site of origin (22–24). Detailed histological analysis of autopsy and surgical tumor tissues from all 3 sites also reveal consistent structural and molecular progression patterns associated with tumor size (22). Smaller tumors ($<8\,mm^3$) show exclusively mesenchymal structures, similar to nerve root DASEs. Tumors with larger volumes ($8–637\,mm^3$) reveal mesenchymal components with some additional epithelioid (i.e. clear cell, cellular) structural features, that is, clustered tumor cells with increased nuclear and cytoplasmic size (resembling stromal cells) and abundant capillaries encompassing these clusters. The largest tumors ($>646\,mm^3$) consistently include mesenchymal and epithelioid structures, frequently with extramedullary hematopoiesis foci exclusively confined to the epithelioid areas. Moreover, mesenchymal structures indicate a MIB1 proliferation index of less than 2%, epithelioid structures with variable MIB1 indices between 3% and 30%, and extramedullary hematopoiesis foci with 100% MIB1 positivity, suggesting an association between proliferative activity and hemangioblastomatous differentiation. Akin to nerve root DASEs, poorly differentiated cells within mesenchymal tumors show nuclear signal for HIF2α, but not HIF1α. Likewise, tumors with mesenchymal and epithelioid components show both HIF1α and HIF2α expression in the epithelioid areas but only HIF2α expression in the mesenchymal areas. The results of HIF immunohistochemistry indicate that the earliest stages of VHL tumorigenesis in the nervous system involve mesenchymal structure with exclusive activation of HIF2α, whereas tumor growth and progression are associated with epithelioid structure and additional activation of HIF1α. Furthermore, constitutive activation of HIF as a result of pVHL deficiency leads to the upregulation of VEGF and CAIX throughout early and late stages of tumor progression, as demonstrated by molecular expression experiments (26). Tumors from the cerebellum and brainstem follow equivalent structural and molecular progression patterns as spinal cord hemangioblastoma (22).

The structural and molecular analyses of hemangioblastomas and particularly of spinal nerve root DASEs in the peripheral nervous system provide the basis for studies of tumorigenesis in the central nervous system proper. We previously reported multiple DASEs in cerebella of VHL patients, with equivalent structural and molecular expression patterns as in spinal nerve root DASEs (Supplementary Data Fig. S1) (9, 25). Briefly, 5 VHL autopsy patients (designated Patients #1–5) and 3 non-VHL (comparative control) autopsy patients were studied. The patient ages, genders, cerebellar hemangioblastomas (antemortem surgical and postmortem resections), and cerebellar DASEs are provided in Table 1. The entire cerebella from all 8 autopsy patients were systematically sectioned. One tissue sample from each section was stained with hematoxylin and eosin (H&E) and then examined under the microscope. Ten cere-

TABLE 1. VHL and non-VHL Adult Autopsy Patients

Patient	Age (Years)	Gender	# Cerebellar HBs Surgically Resected	# Cerebellar HBs at Autopsy	# Cerebellar DASEs
VHL 1	54	Male	1	3	4
VHL 2	17	Female	0	0	3
VHL 3	39	Male	1	0	2
VHL 4	47	Male	1	1	1
VHL 5	26	Female	0	0	0
Control 1	28	Female	0	0	0
Control 2	48	Female	0	0	0
Control 3	49	Male	0	0	0

Demographic features of 5 VHL and 3 non-VHL (comparative control) adult autopsy patients and number of cerebellar hemangioblastomas and DASEs.

VHL, von Hippel-Lindau; DASEs, developmentally arrested structural elements; HB, hemangioblastoma.

bellar DASEs in toto were found in VHL Patients #1–4, with no DASEs identified in VHL Patient #5 or the 3 non-VHL patients (Fig. 1). Three DASEs were identified in Patient #2 (17-year-old female) who had no clinical history of hemangioblastoma. Similar to VHL nerve root DASEs and smaller hemangioblastomas, all 10 cerebellar DASEs had mesenchymal structures, and poorly differentiated cells within DASEs expressed HIF2α and CAIX, but not HIF1α, demonstrating pVHL deficiency. Each cerebellar DASE involved the molecular layer (3 DASEs exclusive to molecular layer), consistent with tumors occupying the cerebellar cortex. Cerebellar DASEs were also mapped topographically to the dorsal cerebellum (2 DASEs peridorsal), where cerebellar hemangioblastomas primarily arise. Taken together, these results (structural and immunohistochemical resemblances to VHL-deficient nerve root DASEs/mesenchymal hemangioblastomas, molecular layer as a consistent site of origin, dorsal cerebellum as a primary location) support these cerebellar DASEs as neoplastic precursors to cerebellar hemangioblastomas.

Here, we provide evidence pointing to developmentally arrested basket/stellate cells as tumor cells of origin. Since the collective data suggest a molecular layer origination for cerebellar hemangioblastoma, 3 hypotheses were formulated. First, the tumor cell of origin is a developmentally arrested hemangioblast that preferentially resides in the molecular layer. Differing from hemangioblastoma, however, cerebellar DASEs do not express brachyury, which does not support this hypothesis (9, 25). Second, the tumor cell of origin is a developmentally arrested neuronal progenitor of the molecular layer, with a retained capacity to proliferate and differentiate into cells with hemangioblast characteristics. The second hypothesis requires investigation into 2 possibilities: granule cell progenitors, which migrate from the external germinal layer through the molecular and Purkinje layers to form the internal granular layer (27), and basket/stellate cell progenitors, which migrate from the inner germinal layer through white matter, the internal granular layer and the Purkinje layer to form the molecular layer (28).

MATERIALS AND METHODS

Human Tissues for Immunohistochemical Analyses

The entire cerebella from 5 VHL patients were collected at autopsy and grossly examined (Table 1) (9, 25). All 5 VHL patients had documented germline mutations in the *VHL* gene. Two VHL patients had hemangioblastomas detectable upon gross examination at autopsy; the macroscopic hemangioblastomas were completely resected and the diagnosis was verified by histological analysis. The remaining cerebellar tissues of these 2 VHL patients, in addition to the cerebella of the other 3 VHL patients, were cut parasagittally into 2-mm slices and then further coronally into $25 \times 30\,mm^2$ segments. All segments were fixed in formalin, embedded in paraffin blocks, and sectioned at a thickness of 6 μm. One cerebellar tissue section from each paraffin block was placed on a glass slide and stained with H&E for initial microscopic examination. Three hundred eighty-five H&E slides for the 5 VHL patients were examined, and 10 DASEs were identified in toto. No tissue sections for DASEs from VHL Patients #3 and 4 were available for further immunohistochemical analysis because their respective paraffin blocks were missing from the tissue archives. The remaining paraffin blocks with a microscopic DASE were serially sectioned at a thickness of 8 μm. At defined intervals of 80 μm, tissues were stained with H&E to confirm that the DASE was contained within the selected interval. Immunohistochemistry experiments were then performed on the unstained, interval tissue sections.

Most tissues for immunohistochemistry were derived from autopsy patients, with the exception of 13 surgically resected cerebellar hemangioblastomas from VHL patients. These tumors were obtained from the Surgical Neurology Branch Tumor Bank Repository. The Tumor Bank contains specimens routinely procured at the time of surgery under IRB Protocol 03N-0164.

Immunohistochemistry

We used the antibodies Zic family member 1 (ZIC1) (rabbit polyclonal antibody, 1:1000 dilution, Abcam, Cambridge, MA, cat. #ab72694), paired box 2 (PAX2) (rabbit polyclonal antibody, 1:500 dilution, Abcam, cat. #ab23799), glial fibrillary acidic protein (GFAP) (mouse monoclonal antibody, 1:200 dilution, DAKO, Carpinteria, CA, cat. #M0761), NMYC downstream-regulated gene 2 (NDRG2) (rabbit polyclonal antibody, 1:150 dilution, Sigma, St. Louis, MO, cat. #HPA002896), CD34 (mouse monoclonal antibody, 1:40 dilution, DAKO, cat. #M7165), platelet/endothelial cell adhesion molecule (PECAM, CD31) (mouse monoclonal antibody, 1:20 dilution, DAKO, cat. #M0823), HIF2α (rabbit polyclonal antibody, 1:10 000 dilution, PM8 antiserum), HIF1α (mouse monoclonal antibody, 1:1000 dilution, Neomarkers, Fremont, CA, cat. #MS-1164), and CAIX (mouse monoclonal antibody, 1:50 dilution, DAKO, cat. #M75). We also used a second PAX2 antibody on 3 surgically resected VHL cerebellar hemangioblastomas (rabbit polyclonal antibody, 1:500 dilution, Lifespan Biosciences, Seattle, WA, cat. #LS-C31501/0859).

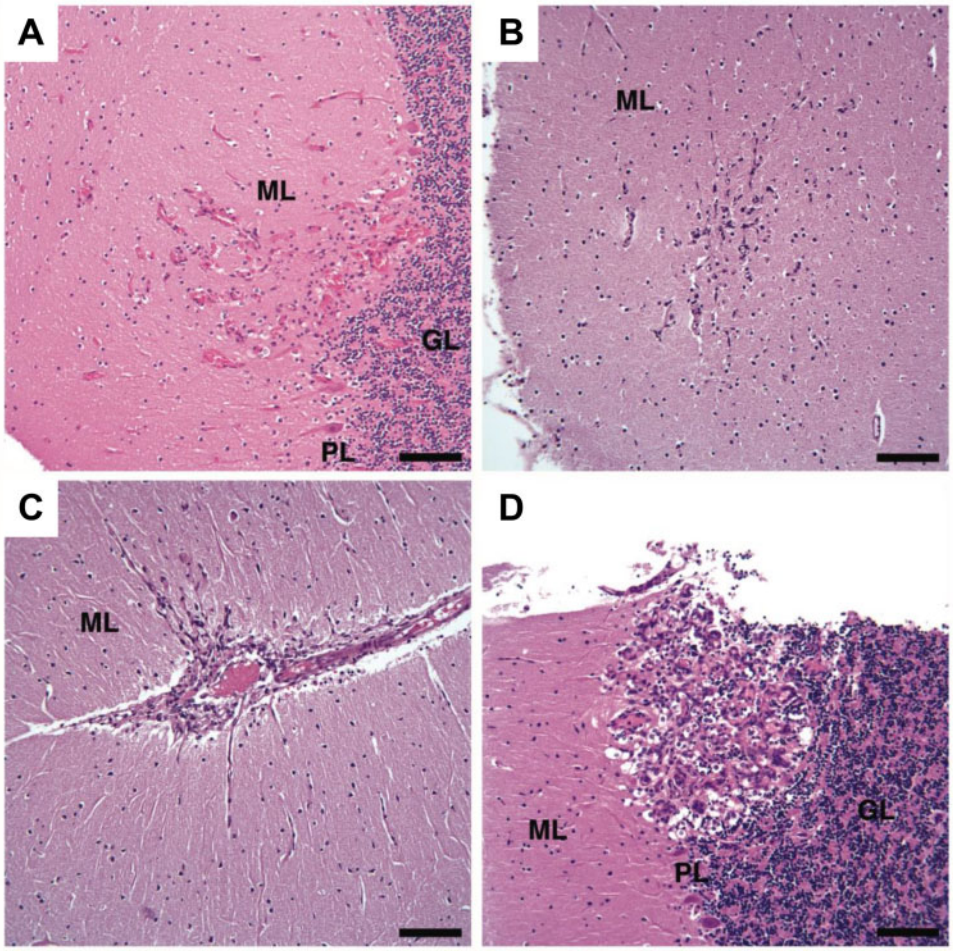

FIGURE 1. H&E stains of the 4 smallest DASEs in cerebellar cortices from VHL patients. **(A)** VHL Patient #1, **(B–D)** VHL Patient #2. H&E, hematoxylin and eosin; DASEs, developmentally arrested structural elements; VHL, von Hippel-Lindau; ML, molecular layer; GL, granular layer; PL, Purkinje layer. Scale bars: **A–D** = 100 μm.

For the immunohistochemistry experiments with ZIC1, NDRG2, and both PAX2 antibodies, we used the following protocol. The sections were deparaffinized with xylene, hydrated with descending concentrations of ethanol solutions, and rinsed with tap water. For antigen retrieval, sections were immersed in sodium citrate buffer (10 mM, pH 6.0) at boiling temperature for 10 minutes and then at room temperature for 30–60 minutes. The sections were then rinsed with tap water. To quench endogenous peroxidase activity, sections were placed in a solution of 0.5% H_2O_2 in methanol for 20 minutes. After 3 washes in Tris-buffered saline (TBS) (pH 7.4), sections were incubated in TBS with 0.1% Triton X-100 for 12 minutes. After another 3 washes in TBS, sections were incubated in block solution, comprised of 10% normal goat serum and 1% bovine serum albumin in TBS, for at least 2 hours. The primary antibody was diluted in block solution. For negative controls, serial tissue sections were treated with rabbit nonimmune IgG (Vector Laboratories, Burlingame, CA, cat. #I-1000), diluted in block solution to be equivalent in concentration to the primary antibody IgG. The sections were incubated in a humidified chamber at 4°C overnight. The next day, the sections were washed in TBS, incubated in TBS with 0.025% Triton X-100 for 5 minutes, and washed again in TBS. Then the sections were incubated with secondary antibody for 45 minutes, followed by avidin-biotin complex incubation for 30 minutes according to the manufacturer's instructions (Vector Laboratories) and then visualization with diaminobenzidine solution (Vector Laboratories). The sections were counterstained with hematoxylin for 5 seconds, dehydrated with ascending concentrations of ethanol solutions, and cleared with xylene before application of Permount and coverslip.

The GFAP, CD34, and CD31 immunohistochemistry experiments were conducted in the Laboratory of Pathology at the National Cancer Institute, according to a clinical protocol. The HIF2α, HIF1α, and CAIX immunohistochemistry experiments were conducted at the Imperial College of Science, Technology and Medicine, as previously described (29).

Oligonucleotide RNA Expression Array

The gene expression microarray experiments required frozen samples approximately 30 mm^3 in size such that micro-

TABLE 2. VHL and non-VHL Patients within Cohorts

Cohort	Cohort #	Age (Years)	Gender	Tumor Size (mm^3)
Pediatric non-VHL cerebellar cortex	1	1.2	Male	Not applicable
		1.3	Male	Not applicable
		2.8	Female	Not applicable
Adult non-VHL cerebellar cortex	2	35	Female	Not applicable
		30	Male	Not applicable
Adult VHL cerebellar cortex	3	42*	Male	Not applicable
		42*	Male	Not applicable
		49	Male	Not applicable
		56	Female	Not applicable
Mesenchymal VHL hemangioblastoma	4	20†	Male	4 × 4 × 2
		20†	Male	9 × 5 × 5
		54	Female	10 × 5 × 4
Epithelioid VHL hemangioblastoma	5	48	Female	20 × 14 × 10
		31	Female	20 × 15 × 15
		30	Female	20 × 15 × 15

Demographic features of patients within each cohort and descriptions of frozen tissues used for gene expression analyses.
VHL, von Hippel-Lindau.
*Two separate samples from same patient.
†Two separate tumors surgically resected from same patient.

scopic, paraffin-embedded cerebellar DASEs could not be used. Three mesenchymal and 3 epithelioid cerebellar hemangioblastomas from 5 other VHL patients were selected. These tumors were also obtained from the Surgical Neurology Branch Tumor Bank Repository. The frozen blocks were sectioned, stained with H&E, and examined under the microscope to confirm the structural classifications of the samples. Additionally, cerebellar cortices from 3 adult VHL, 2 adult non-VHL, and 3 pediatric non-VHL autopsy patients were included. Each tissue category was designated a cohort with a specific number, namely pediatric non-VHL cerebellar cortex [1], adult non-VHL cerebellar cortex [2], adult VHL cerebellar cortex [3], mesenchymal VHL hemangioblastoma [4], and epithelioid VHL hemangioblastoma [5] (Table 2).

We extracted total RNA with TRIzol-reagent (Invitrogen, Carlsbad, CA). The RNA was then purified with the RNeasy Mini kit (Qiagen, Valencia, CA) according to the manufacturer's instructions. The concentration of each RNA sample was determined with the NanoDrop spectrophotometer ND-1000 (NanoDrop Technologies, Wilmington, DE). Before expression analyses, the quality of RNA samples was assessed with an Agilent 2100 Bioanalyzer (Agilent Technologies Inc., Santa Clara, CA). The RNA samples were analyzed with GeneChip Human Genome U133 Plus 2.0 microarrays (Affymetrix, Santa Clara, CA). One GeneChip was used for each tissue sample. An aliquot of 1.5 μg of total RNA from each sample was used. Both cDNA and biotinylated cRNA were synthesized with the Affymetrix GeneChip Expression 3′Amplification One-Cycle Target Labeling and Control Reagent kit according to manufacturer's instructions. Seventeen micrograms of biotinylated cRNA were fragmented and hybridized to Affymetrix Gene-Chips HG U133 Plus2 (Affymetrix) for 16 hours. The arrays were washed and stained on the Affymetrix Fluidics station 400 and scanned with a Hewlett Packard G2500A gene Array Scanner.

We next analyzed the expression profile data. The statistical programming language R was used (http://cran.r-project.org/). Probe-level summarization and expression normalization for 54 675 gene fragments were conducted with the guanine, cytosine nucleotide-rich content correction robust multiarray average (gcRMA) package (http://bioconductor.org) (30). To check for and confirm the absence of sample-level outliers, relationships using the normalized expression for all gene fragments were analyzed with Tukey box plot, covariance-based principal component analysis scatter plot, and Pearson correlation heat map (31–33). To identify and remove gene fragments with noise-biased expression, the coefficient of variation and mean expression per gene fragment per cohort were calculated, and then modeled by cohort via locally weighted scatterplot smoothing (LOWESS). The LOWESS fits were then inspected and the noise threshold was defined as the lowest expression value across fits at which the linear relationship between mean expression (signal) and coefficient of variation (noise) was primarily nullified (noise threshold value = 6). Gene fragments without at least one observed value greater than this noise threshold were then removed from further analysis (33 629 gene fragments), and values for the remaining gene fragments (21 046) were floored to equal the noise threshold if less than the value 6 (34, 35). To test for differential expression, the one-factor analysis of variance was used, with the cohort defined as the factor (36). Gene fragments with Benjamini and Hochberg multiple comparison corrected p value <0.05 (5704 gene fragments) were determined as showing significantly different expression patterns across cohorts (37). The list of gene fragments was further shortened to 3287 with the additional requirement that probe sets be designated _at (antisense). We then individually analyzed the following gene fragments: *HIF2α*, *CAIX*, *ZIC1*, *ZIC2*, meis homeobox 1 (*MEIS1*), *PAX6*, nescient helix loop helix 2 (*NHLH2*, *NSCL2*), neurogenic differentiation 1 (*NEUROD1*), *NEUROD2*, reelin (*RELN*), and astrotactin 1 (*ASTN*). Tukey's Honest Significant (TukeyHSD) test was used to determine significant differences in expression of each gene fragment among the cohorts (uncorrected $\alpha < 0.05$) (38).

RESULTS

VHL Cerebellar DASEs and Hemangioblastomas Do Not Express Granule Cell Progenitor Markers

We first tested the hypothesis that the tumor cell of origin is a developmentally arrested granule cell progenitor. For immunohistochemistry experiments, the cerebellar DASEs and 3 cerebellar hemangioblastomas did not immunoreact with the antibody ZIC1, a zinc finger protein expressed in granule cell progenitors of the external granular layer during the development of human cerebellum (prenatal and postnatal) and also in medulloblastoma (Fig. 2A–C) (39). Additionally, we conducted oligonucleotide RNA expression array experiments with frozen cerebellar tissues from 5 cohorts: pediatric non-VHL cortex, adult non-VHL cortex, adult VHL cortex, mesenchymal VHL

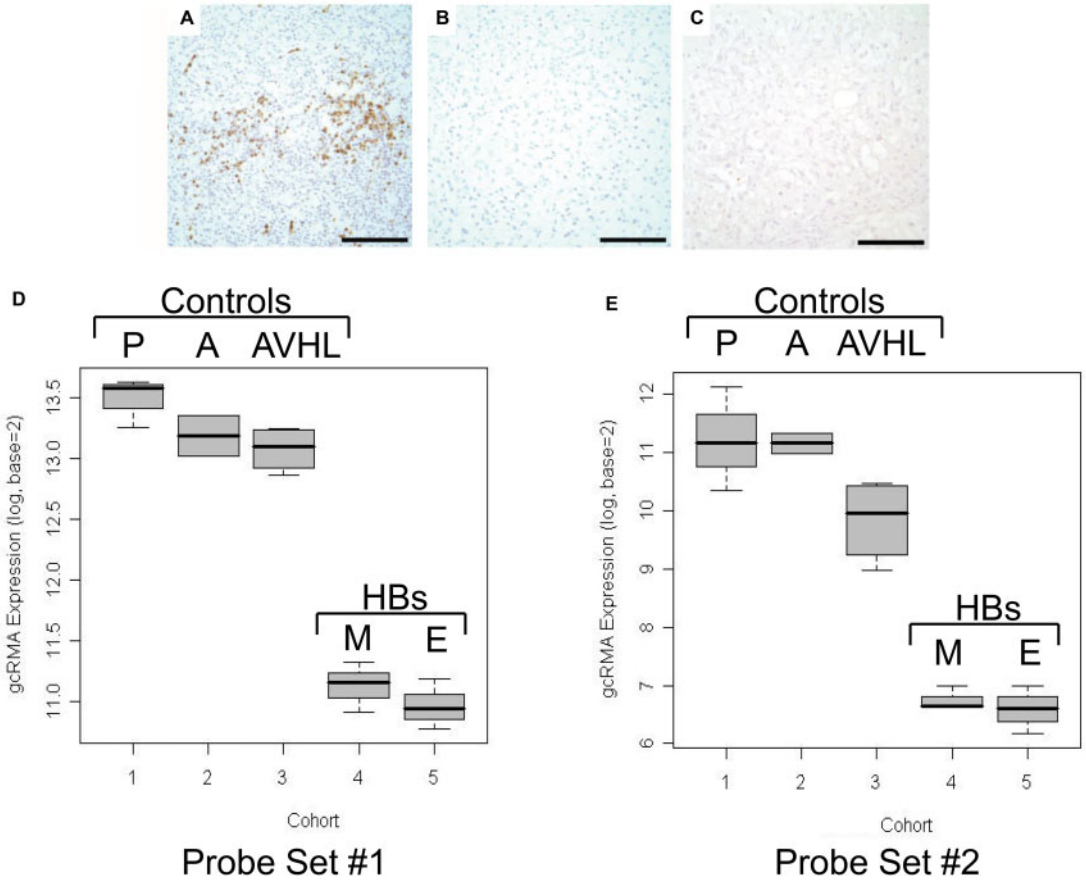

FIGURE 2. Lack of ZIC1 expression in VHL cerebellar HBs and DASEs. ZIC1 immunohistochemistry shows immunoreactivity in **(A)** medulloblastoma as positive control, but no immunoreactivity in **(B)** cerebellar HB or **(C)** cerebellar DASE. **(D, E)** Expression profile data analyses for *ZIC1*. Tukey box plot of gcRMA expression for **(D)** probe set #1 (Affymetrix probe set 206373_at) and **(E)** probe set #2 (Affymetrix probe set 236896_at) show decreased *ZIC1* mRNA expression in mesenchymal and epithelioid VHL HB cohorts in comparison to the 3 cerebellar cortices cohorts. The y-axes show values above the designated noise threshold value of 6. Cohorts: pediatric non-VHL cerebellar cortex (P), adult non-VHL cerebellar cortex (A), adult VHL cerebellar cortex (AVHL), mesenchymal VHL HB (M), epithelioid VHL HB (E). ZIC1, Zic family member 1; VHL, von Hippel-Lindau; DASEs, developmentally arrested structural elements; HBs, hemangioblastomas. Scale bars: **A-C** = 100 μm.

hemangioblastoma, and epithelioid VHL hemangioblastoma, designated cohorts #1–5, respectively. The patient ages, genders, and tumor sizes (when applicable) are provided in Table 2. After the application of summarization, normalization, quality control, noise threshold determination, significance testing methods, and other restrictions, only 3287 gene fragments remained for analysis (from the original 54 675 gene fragments). To test the data and statistical methods, gene expression of molecules prominent in VHL hemangioblastoma, namely *HIF2α* and *KDR* (kinase insert domain receptor, FLK1, VEGFR2), were analyzed to serve as positive controls (11, 12, 14). For both *HIF2α* and *KDR*, the pairwise comparisons among the 5 cohorts showed mRNA expression increased in mesenchymal and epithelioid VHL hemangioblastomas [TukeyHSD post hoc test p values <0.0001 for all comparisons between cerebellar (1–3) and tumor (4, 5) cohorts] (Supplementary Data Fig. S2). Relatively few gene fragments available imposed limitations for analysis (particularly for tumor cell of origin). As such, we searched for genes associated with granule cells, basket/stellate cells, Bergmann glial/astrocytic cells, and Purkinje cells. We identified 10 gene fragments in toto, which all represented granule cells. Two probe sets were antisense *ZIC1* gene fragments. For the first *ZIC1* probe set (206373_at), the pairwise comparisons among the 5 cohorts showed *ZIC1* mRNA expression decreased in mesenchymal and epithelioid VHL hemangioblastomas (TukeyHSD post hoc test p values <0.0001 for all comparisons between cerebellar [1, 2, 3] and tumor [4, 5] cohorts) (Fig. 2D; Table 3). For the second *ZIC1* probe set (236896_at), the pairwise comparisons among the 5 cohorts showed *ZIC1* mRNA expression also decreased in mesenchymal and epithelioid VHL hemangioblastomas (TukeyHSD *post hoc* test p values ranged from 0.0000 to 0.0004 for all comparisons between cerebellar [1, 2, 3] and tumor [4, 5] cohorts) (Fig. 2E; Table 3). The decreased *ZIC1* mRNA expression in VHL hemangioblastomas corroborated the results of the immunohistochemistry experiments that showed a lack of ZIC1 protein expression in VHL cerebellar DASEs and tumors. Gene expression analyses revealed that the

TABLE 3. Expression Profile Data Analyses for *ZIC1* Probe Sets

Comparison	Probe Set #1		Probe Set #2	
	Fold Change	Tukey p Value	Fold Change	Tukey p Value
2*v*1	−1.2320	0.5142	−1.0422	1.0000
3*v*1	−1.3285	0.1339	−2.5916	0.0792
4*v*1	−5.1247	<0.0001	−22.0827	<0.0001
5*v*1	−5.7418	<0.0001	−24.6785	<0.0001
3*v*2	−1.0783	0.9685	−2.4866	0.1604
4*v*2	−4.1596	<0.0001	−21.1881	0.0001
5*v*2	−4.6604	<0.0001	−23.6787	0.0001
4*v*3	−3.8574	<0.0001	−8.5209	0.0004
5*v*3	−4.3218	<0.0001	−9.5226	0.0003
5*v*4	−1.1204	0.8535	−1.1175	0.9971

Pairwise comparisons among the 5 cohorts with fold changes and corresponding TukeyHSD post hoc test p values (p values < 0.05 considered significant). The 5 cohorts: pediatric non-VHL cerebellar cortex [1], adult non-VHL cerebellar cortex [2], adult VHL cerebellar cortex [3], mesenchymal VHL hemangioblastoma [4], and epithelioid VHL hemangioblastoma [5]. Probe set #1 (Affymetrix probe set 206373_at), probe set #2 (Affymetrix probe set 236896_at).

ZIC1, Zic family member 1; TukeyHSD, Tukey's Honest Significant Differences; VHL, von Hippel-Lindau; at, antisense; *v*, versus.

other 8 genes critical to the granule cell lineage (*ZIC2*, *MEIS1*, *PAX6*, *NHLH2*, *NEUROD1*, *NEUROD2*, *RELN*, and *ASTN*) were similarly expressed at significantly lower levels in the hemangioblastoma cohorts than in the cerebellar cortex cohorts (Supplementary Data Figs. S3 and S4). Thus, the combined microarray and immunohistochemistry data did not support the hypothesis of granule cell progenitor as tumor cell of origin.

VHL Cerebellar DASEs and Hemangioblastomas Express Basket/Stellate Progenitor Marker PAX2

We then tested the hypothesis that the tumor cell of origin is a developmentally arrested basket or stellate cell, gamma–aminobutyric acid (GABA)ergic interneurons, which occupy the molecular layer during development and throughout life (28). In the mouse, Pax2 is a transcription factor and standard marker for identifying basket and stellate cells migrating and differentiating in the molecular layer of the developing cerebellar cortex (40, 41). Poorly differentiated cells within all the cerebellar DASEs and fifteen cerebellar hemangioblastomas (15/15) showed nuclear immunoreaction with PAX2 antibody in immunhistochemistry experiments (Fig. 3A–C). We also used a second antibody to test for immunoreactivity in 3 of the surgically resected VHL cerebellar hemangioblastomas, which similarly showed poorly differentiated cells expressing PAX2 in all tumor samples (Fig. 3D).

VHL Cerebella Express Basket/Stellate Progenitor Marker PAX2 in Purkinje/Molecular Layers

VHL cerebellar tissue samples also revealed nuclear PAX2 immunoreactivity in cells between Purkinje cell somata with extension into the molecular layer consistently throughout the tissue sections on the slides. This molecular and histological pattern partially resembles Pax2 expression of developing basket/stellate cells in the developing mouse cerebellum during postnatal days 5–15 (P5–15) (40, 41). At approximately P5, Pax2-positive cells nestle between and just above the Purkinje cell somata before migrating to the outer superficial molecular layer just below the remains of the external granular layer. By P15, Pax2-positive cells are confined to the outer limit, and the total number of Pax2-positive cells decreases. Pax2 is not expressed in the nervous system of adult mouse. Therefore, we investigated the possibility that the adult VHL cerebellum abnormally contains developmentally arrested basket/stellate cell progenitors in the Purkinje and molecular layers.

We tested cerebellar cortex tissue samples from VHL Patients #1–5, in addition to another VHL patient (Patient #6, 71-year-old male with cerebellar hemangioblastomas), and from 3 adult non-VHL patients with no history of neurological disease (30-year-old male, 35-year-old female, and 53-year-old female) for immunoreactivity with PAX2 antibody. The cerebella from VHL patients #1–4 and 6 showed PAX2 nuclear immunoreactivity in cells between the Purkinje cell somata and in the contiguous molecular layer; all these VHL patients had a history of cerebellar hemangioblastoma (VHL Patients #1, 3, 4, 6) and/or detection of cerebellar DASEs (VHL Patients #1–4) (Fig. 3E). In contrast, the cerebellar cortex of VHL Patient #5 showed no PAX2 immunoreactivity, and this patient had no history of cerebellar hemangioblastoma or detection of cerebellar DASEs (Fig. 3F). Cerebellar cortical tissues from the 3 adult non-VHL patients displayed no PAX2 expression (Fig. 3G). H&E stains revealed no apparent histological differences between adult non-VHL and VHL cerebellar cortices (Fig. 3H, I). Lastly, PAX2-positive cells in VHL cerebellar cortex showed normal vascularization without HIF2α, HIF1α, or CAIX immunohistochemical protein expression (Fig. 4).

Postnatal Human Non-VHL Cerebella Express Basket/Stellate Progenitor Marker PAX2 in Purkinje/Molecular Layers

Little is known about the postnatal development of the molecular layer in the human cerebellum. Santiago Ramón y Cajal studied neuronal perikarya and fibers, stained with the Golgi method, in the molecular layer of adult human, cat, dog, guinea pig, rabbit, chicken, and sparrow cerebella (42, 43). He described basket cells primarily located in the inner third of the molecular layer, which form thick plexuses of terminal arborizations around the cell bodies of Purkinje cells. In contrast, stellate cells primarily occupy the superficial third of the molecular layer, with their dendrites and axons confined to the molecular layer. PAX2 expression in the developing human cerebellum has not been reported.

Therefore, to determine whether PAX2 protein is expressed in cells of the Purkinje and molecular layers during the development of the molecular layer in humans, 10 non-VHL cerebellar cortices from infant and pediatric autopsy patients, ranging in age from 5 days to almost 6 years, were tested for immunoreactivity with PAX2 antibody (Table 4).

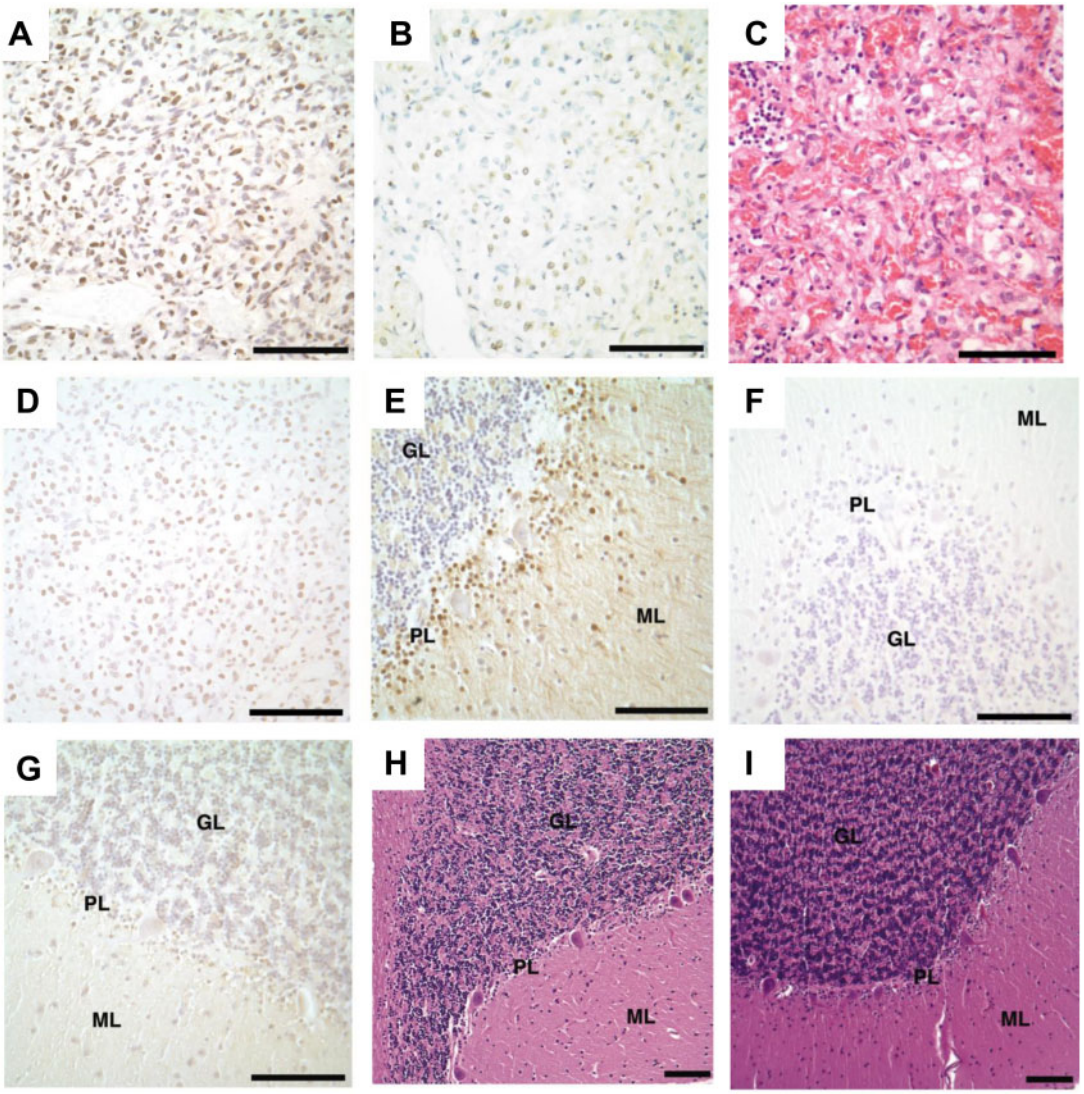

FIGURE 3. PAX2 immunoreactivity in VHL cerebellar hemangioblastomas, DASEs and cortices. PAX2 immunohistochemistry shows immunoreactivity in **(A)** hemangioblastoma. Nonserial tissue sections of DASE show (**B**) PAX2 immunoreactivity and (**C**) H&E stain. Immunohistochemistry similarly shows immunoreactivity with the second PAX2 antibody in (**D**) hemangioblastoma. PAX2 immunohistochemistry shows immunoreactivity in **(E)** VHL cerebellar cortices from Patients #1–4 and 6, but no immunoreactivity in (**F**) VHL cerebellar cortex from Patient #5 and (**G**) adult non-VHL patients. H&E stains show no histological differences between adult **(H)** VHL and **(I)** non-VHL cerebellar cortices. PAX2, paired box 2; VHL, von Hippel-Lindau; DASEs, developmentally arrested structural elements; H&E, hematoxylin and eosin; ML, molecular layer; GL, granular layer; PL, Purkinje layer. Scale bars: **A-I** = 100 μm.

These patients had no clinical history of VHL or neurological diseases. Cerebella from the 3 youngest patients (0 year, 5 days; 0 year, 98 days; and 1 year, 78 days) showed no PAX2 immunoreactivity (Fig. 5A, D, G). Rather, cerebella from the next 6 eldest patients (1 year, 123 days; 1 year, 222 days; 1 year, 259 days; 2 years, 4 days; 2 years, 286 days; and 2 years, 305 days) showed PAX2 immunoreactivity in cells between Purkinje cell somata and contiguous molecular layer consistently throughout the tissue sections on the slides, resembling the PAX2 immunoreactivity pattern in VHL cerebella. (Fig. 5B, E, H). Nevertheless, the cerebellum of the eldest patient (5 years, 343 days) showed no PAX2 immunoreactivity (Fig. 5C, F, I). In summary, PAX2-positive cells were detected in Purkinje and molecular layers of the human cerebellum between the ages of approximately 1 and 3 years, with no PAX2 immunoreactivity by 6 years, similar to the expression pattern of Pax2 between P5 and P15 in mouse cerebellum (40, 41).

VHL Cerebellar DASEs Do Not Express NDRG2 or GFAP

Because Bergmann glial cells also reside in the Purkinje layer and hemangioblastomas can express astrocytic markers,

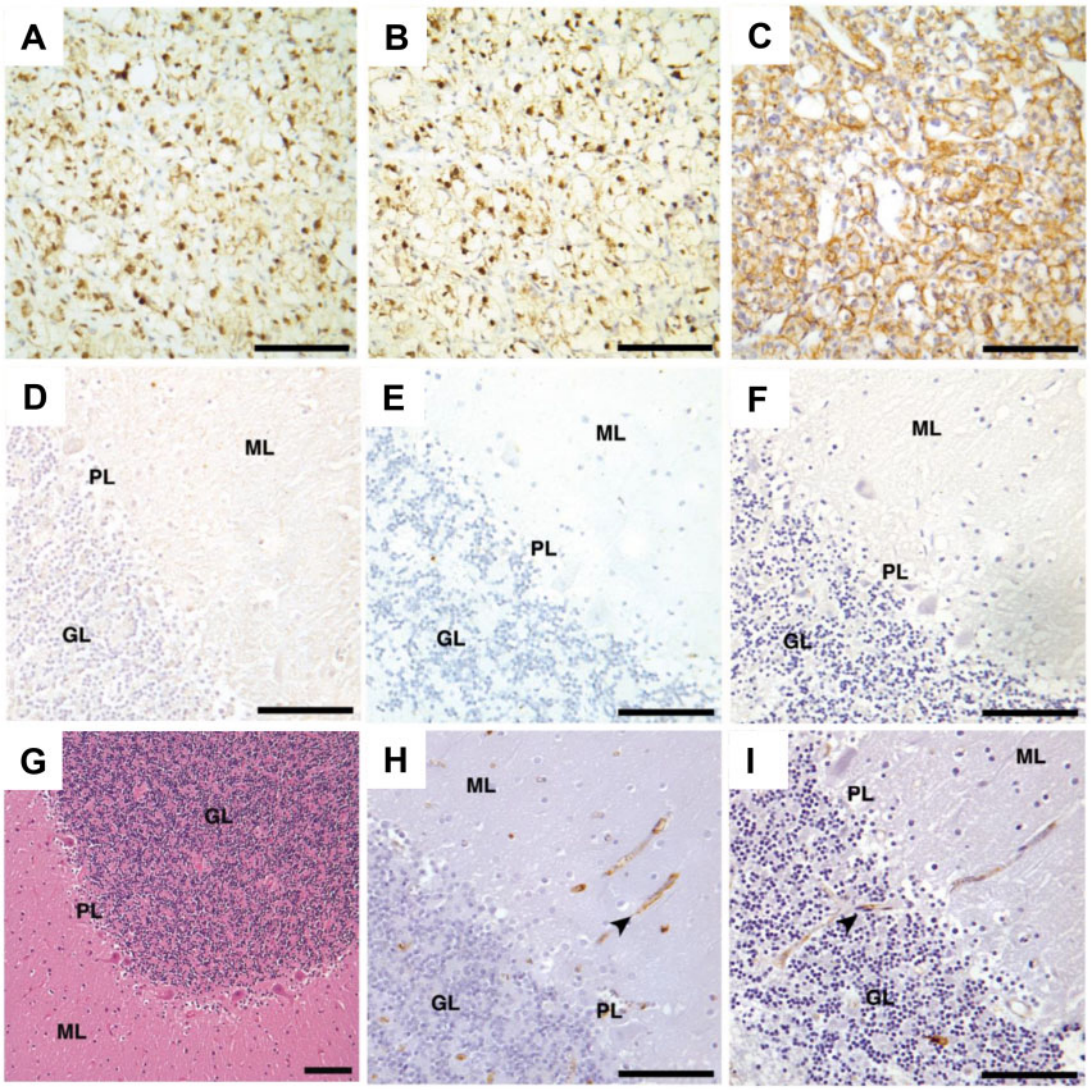

FIGURE 4. VHL cerebellar cortex shows normal vascularization and lack of HIF2α, HIF1α, and CAIX immunoreactivity. Immunohistochemistry shows immunoreactivity in VHL renal clear cell carcinoma as positive controls for (**A**) HIF2α, (**B**) HIF1α, and (**C**) CAIX. Serial tissue sections of VHL cerebellar cortex show no immunoreactivity with (**D**) HIF2α, (**E**) HIF1α, and (**F**) CAIX antibodies. VHL cerebellar cortex shows normal histology and vascularization (arrowhead) with (**G**) H&E stain and (**H**) CD34 and (**I**) CD31 immunohistochemistry. VHL, von Hippel-Lindau; HIF2α, hypoxia-inducible factor 2 alpha subunit; HIF1α, hypoxia-inducible factor 1 alpha subunit; CAIX, carbonic anhydrase IX; H&E, hematoxylin and eosin; ML, molecular layer, GL, granular layer, PL, Purkinje layer. Scale bars: **A-I** = 100 μm.

the possibility that the tumor cell of origin is a Bergmann glial cell was also investigated (28). NDRG2 is a marker for Bergmann glial cells in mouse cerebellum (44). Since NDRG2 expression in Bergmann glial cells of the human cerebellum is unknown, we performed immunohistochemistry experiments with NDRG2 antibody on cerebellar cortex samples from 3 adult non-VHL, 3 pediatric non-VHL (1 year, 78 days; 1 year, 123 days; and 2 years, 286 days) and the 5 VHL patients. Nuclear NDRG2 immunoreactivity was detected in cells among Purkinje cell somata in all cerebellar cortex samples, differing from the PAX2 immunoreactivity results (Fig. 6A–G). In addition, immunohistochemistry experiments showed DASEs immunoreacting with neither the antibody NDRG2 nor GFAP, a marker for astrocytes (Fig. 6H–K). Given Bergmann glial cell somata do not principally occupy the molecular layer during development or in adult life and the lack of DASE immunoreactivity, the evidence does not support the hypothesis of Bergmann glial cell as tumor cell of origin (43, 45–47).

DISCUSSION

VHL hemangioblastomas express neuronal markers, including neuron-specific enolase (gamma-enolase) and neural cell adhesion molecule (CD56) (9, 48, 49). Since cerebellar DASEs consistently dwell in molecular layer and do not express mesodermal hemangioblast marker brachyury, we tested

TABLE 4. Infant and Pediatric non-VHL Autopsy Patients

Age	Gender	PAX2
0 year, 5 days	Male	−
0 year, 98 days	Male	−
1 year, 78 days	Male	−
1 year, 123 days	Male	+
1 year, 222 days	Male	+
1 year, 259 days	Male	+
2 years, 4 days	Female	+
2 years, 286 days	Female	+
2 years, 305 days	Male	+
5 years, 343 days	Female	−

Demographic features of infant and pediatric non-VHL autopsy patients and PAX2 immunoreactivity in cerebellar cortices.

+, positive immunoreactivity; −, negative immunoreactivity; VHL, von Hippel-Lindau; PAX2, paired box 2.

the hypothesis that the cerebellar tumor cell of origin is a developmentally arrested neuronal progenitor of the molecular layer with the retained capacity to proliferate and differentiate into cells with hemangioblast phenotype. One candidate is the granule cell progenitor, which migrates through the molecular layer during development (27). The oligonucleotide RNA expression array and immunohistochemistry results, however, did not support this hypothesis. For gene expression analyses, 9 molecular markers associated with granule cell development (*ZIC1*, *ZIC2*, *MEIS1*, *PAX6*, *NHLH2*, *NEUROD1*, *NEUROD2*, *RELN*, and *ASTN*) revealed significantly decreased expression in the 2 hemangioblastoma cohorts in comparison to the 3 cerebellar cortex cohorts. The immunohistochemistry experiments showed that cells within the cerebellar tumors did not express ZIC1, thereby directly corroborating the microarray analyses for this particular marker. Also, cells within the cerebellar DASEs did not express ZIC1. The other neuronal progenitor candidates are the basket and stellate cells, GABAergic interneurons that occupy the molecular layer during development and throughout life (28). Pax2 is a standard marker for identifying basket and stellate cells migrating and differentiating in the molecular layer of the developing mouse cerebellar cortex, including P5-P15 (40, 41). Cells within all DASEs and tumors immunoreacted with PAX2 antibodies, as well as cells in the Purkinje layer with extension into the molecular layer in the cerebellum of all VHL patients with cerebellar hemangioblastomas and/or DASEs. We further sketched that the postnatal human non-VHL cerebellum expresses PAX2 in cells of the Purkinje and molecular layers (likely between the approximate ages of 1 and 5 years), similar to the temporal pattern in the mouse.

We propose that the cerebellar tumor cells of origin in VHL disease are basket/stellate cell progenitors in the molecular and Purkinje layers of the cerebellar cortex, developmentally arrested at a young, postnatal age. Cells expressed PAX2 in postnatal human non-VHL cerebellum at equivalent positions as adult VHL and postnatal murine cerebella, suggesting both that the human cerebellum undergoes similar PAX2 expression and molecular layer development as the mouse and that in the VHL cerebellum, the developmental process arrests. Also similar to mouse, adult non-VHL cerebellum did not display PAX2-positive cells. H&E and immunohistochemistry results revealed differences between adult non-VHL and VHL cerebella not by structure, but rather by differential molecular expression of PAX2. Interestingly, we also identified PAX2 expression in all brainstem (5/5) and spinal cord (9/9) hemangioblastoma tissue samples, in addition to one spinal nerve root DASE (1/1) (Supplementary Data Fig. S5) (9, 50). Since mouse GABAergic interneurons require Pax2 for differentiation in the developing dorsal spinal cord, we analogously hypothesize that spinal cord—and probably brainstem—hemangioblastomas in the VHL patient likewise originate from developmentally arrested GABAergic interneurons in specific, consistent histological sites (e.g. nerve root) (51, 52). Though we did not have these tissue samples, VHL retinal hemangioblastoma should also be tested for PAX2 expression, as well as identification of sites of origin for both brainstem and retinal tumors. Whether the PAX2-positive cells in VHL cerebellum are haploinsufficient or have lost the wild-type *VHL* allele is another critical question. Nonetheless, either equipped with one intact wild-type *VHL* allele or none, cells expressing PAX2 should not reside in adult cerebellum (40, 41).

The consistent PAX2 expression in VHL cerebella, DASEs, and tumors also provides a molecular link in the progression model for hemangioblastoma (Fig. 7). Due to *VHL* gene deficiency (whether haploinsufficient or with LOH), basket/stellate cells, likely still expressing PAX2, developmentally arrest in the Purkinje and molecular layers, thereby aberrantly residing as a plethora of initiated cells. These cells do not express HIF1α, HIF2α, or CAIX and show no evidence of abnormal, extensive vascularization. With another, as yet unidentified insult or signal, an initiated, immature basket/stellate cell gains the ability to proliferate, forming a DASE composed of pVHL-deficient cells (9, 25). Even though preliminary data suggest dispersion of PAX2-positive cells throughout VHL cerebellar cortex, DASEs (and approximately 75% of tumors) preferentially distribute in dorsal cerebellum (9, 25, 53). Cytologically, poorly differentiated cells within DASEs tend to have little cytoplasm and small nuclei (9, 25). They also express HIF2α and its downstream targets CAIX and VEGF (data not shown), which elicits an angiogenic response from the surrounding cerebellum. The reactive capillaries entwine the poorly differentiated cells. DASEs can further proliferate to form frank tumor (mesenchymal hemangioblastoma) (22). The tumor continues to express HIF2α, CAIX, and VEGF as well as acquires the ability to express other molecules, such as the hemangioblast marker brachyury (16, 22). The tumor cells attempt to form blood vessels and nascent red blood cells, hence the name "hemangioblastoma" (15, 19, 20, 22, 24). Only in the epithelioid form, with the clustering of cells with large nuclei and clear cytoplasm, does the tumor express HIF1α and potentially form foci of extramedullary hematopoiesis (22, 24).

Interestingly, no PAX2-positive cells were detected in the Purkinje and molecular layers of the cerebellum in Patient #5. She died at 26 years of age and had no clinical history of hemangioblastoma. Although no DASEs in the tissue sam-

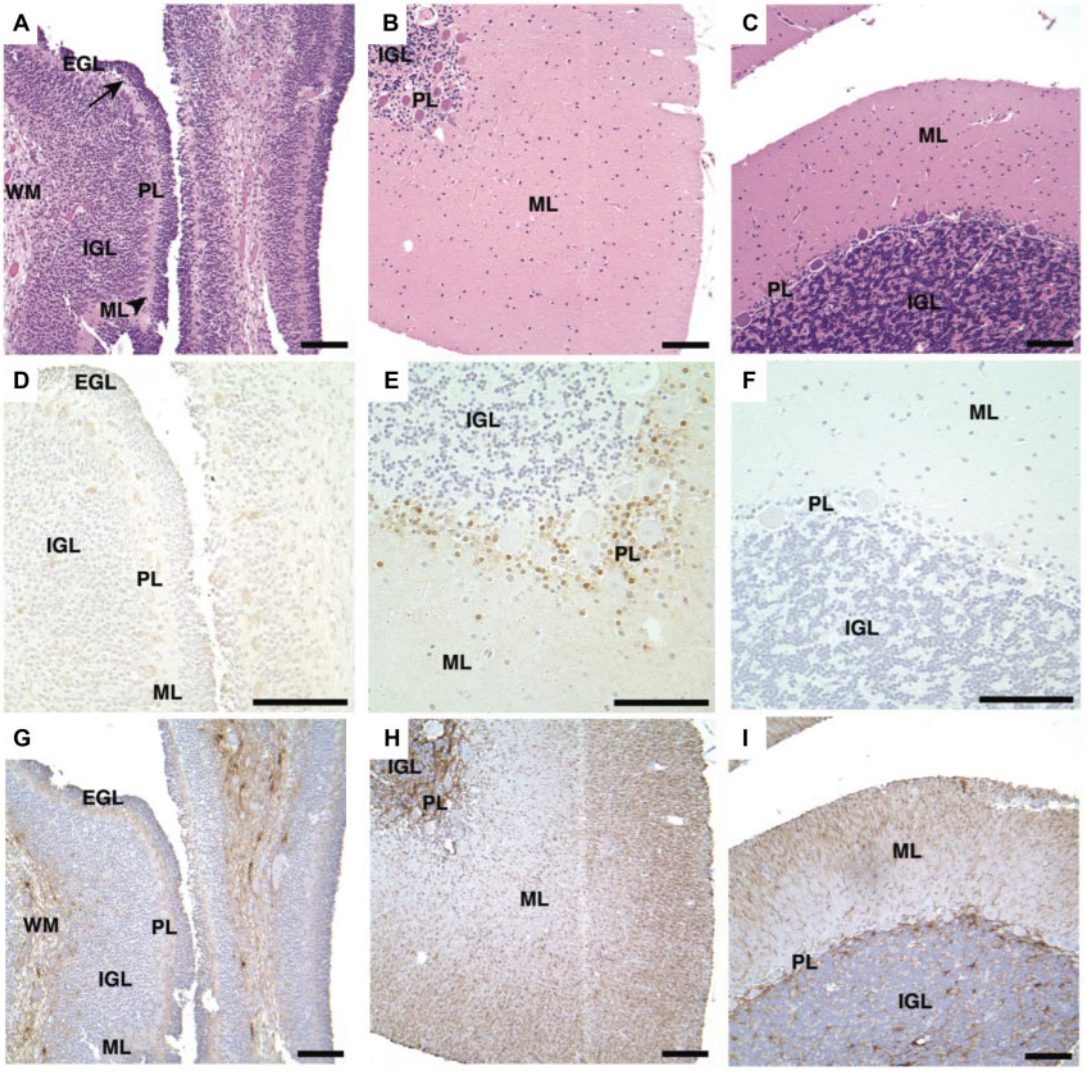

FIGURE 5. PAX2 immunohistochemistry in infant and pediatric non-VHL cerebellar cortices. H&E stains of cerebellar cortex tissues for **(A)** infant non-VHL patient (5 days old), **(B)** pediatric non-VHL patient (2 years, 4 days), and **(C)** pediatric non-VHL patient (5 years, 343 days). Serial tissue sections of PAX2 immunohistochemistry show immunoreactivity in the **(E)** pediatric patient of 2 years, but not the (**D**) infant or (**F**) eldest pediatric patient. Serial tissue sections of GFAP immunohistochemistry indicate tissue integrity (**G-I**). PAX2, paired box 2; VHL, von Hippel-Lindau; H&E, hematoxylin and eosin; EGL, external granular layer (arrow); IGL, internal granular layer; GL, granular layer; ML, molecular layer (arrowhead), PL, Purkinje layer; WM, white matter. Scale bars: **A-I** = 100 μm.

pling of cerebellum were identified, she did, however, have 3 DASEs in the nerve roots of her spinal cord. Tumors in VHL patients can occur in any sequence or combination throughout their lifetimes (4). The VHL patient population develops cerebellar hemangioblastomas at an estimated frequency of 44%–72%, with the mean age of onset at 33 years of age (range 9–78 years) (21). Without PAX2-positive cells, Patient #5 perhaps did not have the potential to develop cerebellar hemangioblastoma.

VHL may normally function as a critical development gene in specific cells at particular times and locations. Currently, *VHL* is considered a gatekeeper tumor suppressor gene with multiple functions, including transcriptional regulation (54). Richards et al (55) showed expression of *VHL* mRNA in human embryos with in situ hybridization at 4, 6, and 10 weeks after conception. They described *VHL* mRNA expression as predominant in the central nervous system, dorsal root ganglion, kidney, testis, and lung. Although the authors noted an inexact correlation between *VHL* mRNA expression in specific topographic sites of the human embryo and the organs in which VHL tumors arise, they proposed that VHL has a role in normal human development. Shortly thereafter, it was shown that VHL promotes differentiation toward a neuronal phenotype in cell culture of rat embryonic day 12 progenitor cells from forebrain and hindbrain and of human neuroblastoma cells (56, 57). In other papers, authors showed that VHL also regulates the extracellular matrix, and of particular interest, fibronectin, essential for the migration of neurons during development (58–64). Fi-

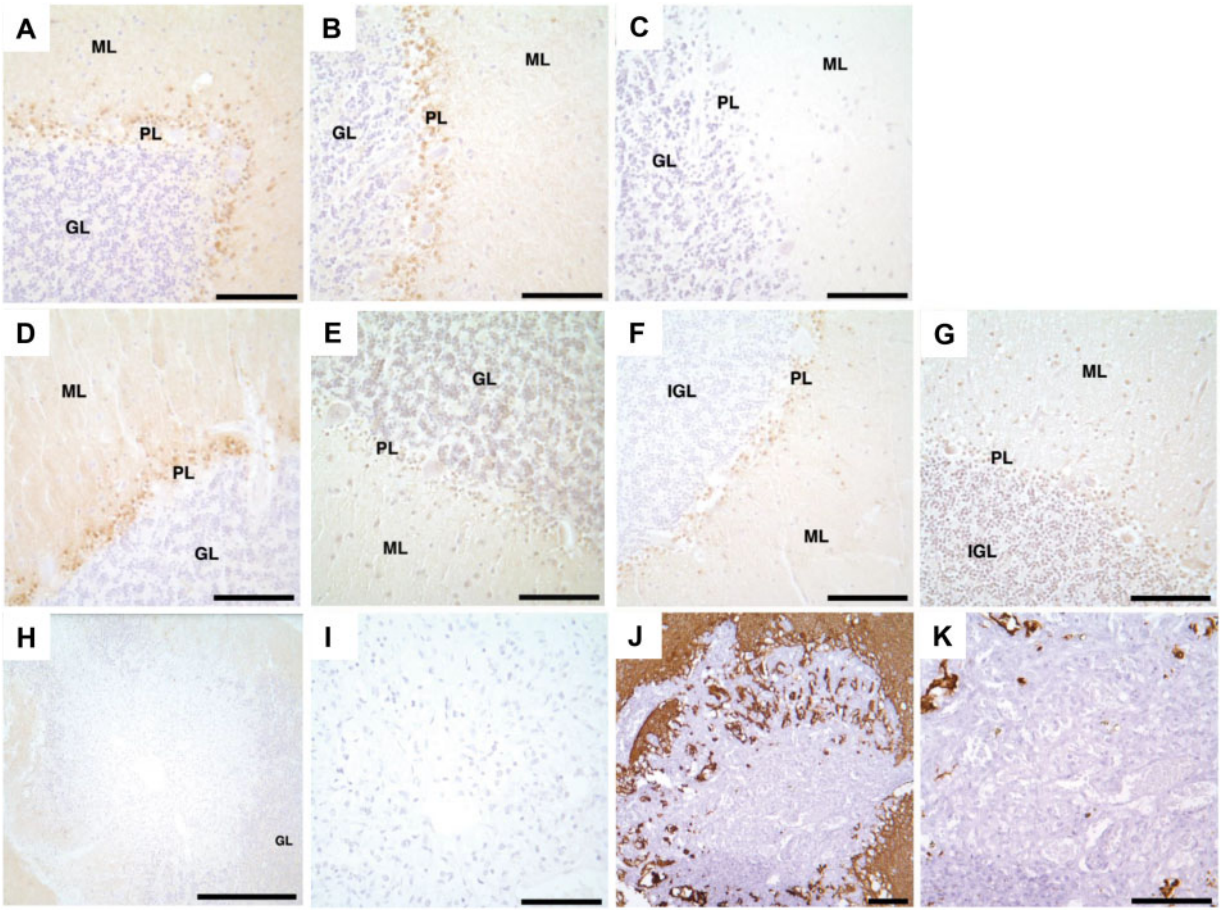

FIGURE 6. NDRG2 immunoreactivity in adult VHL, adult non-VHL and pediatric non-VHL cerebellar cortices, but not VHL cerebellar DASEs. NDRG2 immunohistochemistry shows immunoreactivity in (**A**) adult VHL including (**B**) Patient #5, (**D**) adult non-VHL, and (**F**) pediatric non-VHL (1 year, 78 days) cerebellar cortices. In contrast, PAX2 immunohistochemistry shows no immunoreactivity in (**C**) VHL Patient #5, (**E**) adult non-VHL, and (**G**) early pediatric non-VHL (1 year, 78 days) cerebellar cortices. VHL cerebellar DASEs do not indicate (**H, I**) NDRG2 or (**J, K**) GFAP immunoreactivity. NDRG2, NMYC downstream-regulated gene 2; VHL, von Hippel-Lindau; DASEs, developmentally arrested structural elements; PAX2, paired box 2; GFAP, glial fibrillary acidic protein; GL, granular layer; ML, molecular layer; PL, Purkinje layer. Scale bars: **A–G, I–K** = 100 μm; **H** = 500 μm.

nally, recent data indicate pVHL negatively regulates PAX2, possibly without HIF (65, 66). *PAX* genes encode transcription factors involved in organogenesis, harboring potential for cell programming, such as proliferation, transdifferentiation, and migration (67). Organs associated with VHL tumors normally express Pax2 at various developmental stages (cerebellum, dorsal spinal cord, brainstem, retina, endolymphatic duct, pancreas, adrenal medulla, epididymis, and kidney), suggesting a molecular interaction between VHL and PAX2 gone awry during development in VHL patients (40, 41, 51, 52, 68–71). The concept that VHL is involved in human development, particularly in possible relation to PAX2 during GABAergic interneuronal differentiation/migration, supports the specific proposal that with *VHL* gene deficiency, basket/stellate cell progenitors in the Purkinje and molecular layers undergo developmental arrest in the postnatal cerebellum. These cells then await another insult or signal that triggers proliferation and differentiation in the microenvironmental context of a more developed, *VHL*-haploinsufficient cerebellum. The result is a mass of pVHL-deficient neoplastic cells communicating errant signals with a mismatched microenvironment, otherwise known as hemangioblastoma.

This proposed function of VHL in human development provides a potential explanation for organ specificity, and perhaps tumor specificity as well, in VHL disease. If VHL serves as a critical molecule determining further migration and differentiation in particular cells, such as basket/stellate cells, then the formation of tumor would be specific to that organ, such as the cerebellum. Furthermore, these cells would be arrested at a particular time and site during development. The rest of the organ continues to mature, ultimately placing these developmentally arrested cells in a microenvironment normally separated by time. The interaction of these developmentally arrested cells in a specific, foreign microenvironment may occasion the formation of a specific tumor with consistent structural and molecular progression patterns. The results from this study suggest that developmentally arrested basket/stellate cells in the further developed, *VHL*-haploinsufficient cerebellum have the poten-

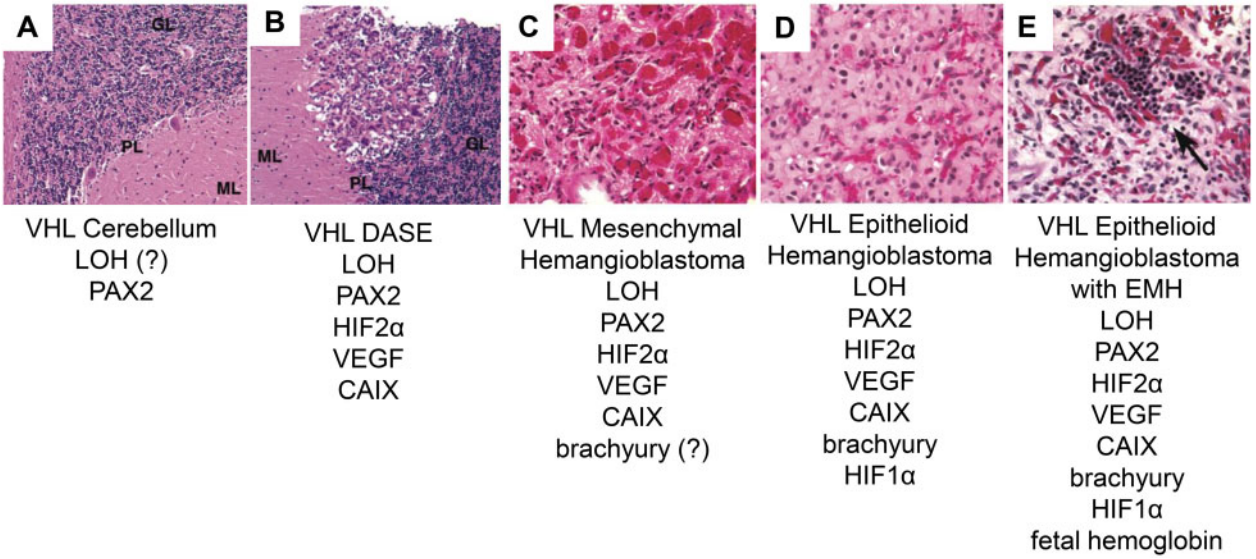

FIGURE 7. Structural and molecular progression model for VHL cerebellar hemangioblastoma. (**A**) VHL cerebellum with PAX2-positive developmentally arrested basket/stellate cells throughout cerebellar cortex. (**B**) VHL DASE with LOH, HIF2α, VEGF, and CAIX. (**C**) VHL mesenchymal hemangioblastoma possibly expressing brachyury. (**D**) VHL epithelioid hemangioblastoma with brachyury and HIF1α. (**E**) VHL epithelioid hemangioblastoma with EMH expressing fetal hemoglobin (arrow). This model is not comprehensive. VHL, von Hippel-Lindau; PAX2, paired box 2; DASEs, developmentally arrested structural elements; LOH, loss of heterozygosity; ?, not determined; HIF2α, hypoxia-inducible factor 2 alpha subunit; VEGF, vascular endothelial growth factor; CAIX, carbonic anhydrase IX; HIF1α, hypoxia-inducible factor 1 alpha subunit; EMH, extramedullary hematopoiesis.

tial to proliferate and differentiate into pVHL-deficient, hemangioblast-like cells with the capacity to instigate angiogenesis, undergo vasculogenesis and form nascent red blood cells with fetal hemoglobin (15, 19, 20, 22, 24).

Understanding the early effects of *VHL* gene deficiency in the formation of hemangioblastoma in the cerebellum may aid in the development of a therapeutic intervention to prevent the progression of precursor to clinically significant hemangioblastoma in the VHL patient. Further study of VHL hemangioblastoma formation may additionally provide insight into the process of tumorigenesis in other VHL tumors; for example, renal clear cell carcinoma with mutated *VHL* gene and endolymphatic sac tumor with 3p loss can express PAX2 protein (65, 72). Likewise, VHL hemangioblastoma formation may serve as a model for tumorigenesis of sporadic, *VHL*-deficient hemangioblastoma and renal clear cell carcinoma, elucidating the processes of initiation and progression in persons of the general population. Concepts elucidated with the study of VHL disease (e.g. DASEs, also reported in VHL endolymphatic duct/sac, epididymis, kidney) most likely will analogously apply to other tumor suppressor syndromes such as BRCA1 (breast cancer gene 1) (29, 73–76). Finally, molecular targets with more precise discernment between tumor and normal cells offer the potential for further diagnostic and therapeutic advancements. Identification of embryological or developmental molecules expressed uniquely by tumor cells supports the principle that tumor and normal cells could be differentiated by time. That is, if tumor cells express molecules once essential during development and no longer expressed by normal cells of an older person, then there exists the possibility of developing specific, molecular targets for diagnosis and therapeutic strategy against those tumor cells.

Conclusion

This study of human tissues from VHL patients provides evidence that *VHL* gene deficiency can result in the developmental arrest of basket/stellate cells in the Purkinje and molecular layers of cerebellum, which can then potentially proliferate and differentiate into hemangioblastoma in a temporally misaligned microenvironment later in the patient's life. If normally dependent on *VHL* gene function at critical time points, specific cells may undergo developmental arrest consequent of *VHL* gene deficiency. This phenomenon hypothetically explains the occurrence of consistent tumor types arising in distinct organ systems associated with VHL disease, such as cerebellar and spinal cord hemangioblastomas and renal clear cell carcinoma, with analogous implications for other tumor suppressor syndromes.

ACKNOWLEDGMENTS

We dedicate this research project to Edward Hudson Oldfield, MD, former Chief of the Surgical Neurology Branch (SNB) at the National Institutes of Health (NIH). SBS was a doctoral student in the Molecular and Cellular Oncology Program of the Institute for Biomedical Sciences at George Washington University and the Graduate Partnerships Program at the NIH. This work was from a dissertation presented to George Washington University in partial fulfillment of the requirements for the PhD degree. We are grateful to Anne Chiaramello for her intellectual insights and support and to

Erich Roessler and Maximilian Muenke at the National Human Genome Research Institute (NHGRI). We would also like to thank Cynthia Harris and Mark Raffeld at the National Cancer Institute (NCI), and Maxine Tran and Patrick Maxwell at the Imperial College of Science, Technology and Medicine, for their expertise in immunohistochemistry protocols. Human tissues were obtained from the Surgical Neurology Branch Tumor Bank Repository at NINDS, Autopsy Service of the Laboratory of Pathology at NCI, and Eunice Kennedy Shriver National Institute of Child Health and Human Development (NICHD) Brain and Tissue Bank for Developmental Disorders at the University of Maryland. The role of the NICHD Brain and Tissue Bank is to distribute tissue and therefore cannot endorse the studies performed or the interpretation of results. The content is solely the responsibility of the authors and does not necessarily represent the official views of the NIH.

REFERENCES

1. Kim WY, Kaelin WG. Role of VHL gene mutation in human cancer. J Clin Oncol 2004;22:4991–5004
2. Knudson AG. Mutation and cancer: Statistical study of retinoblastoma. Proc Natl Acad Sci USA 1971;68:820–3
3. Latif F, Tory K, Gnarra J, et al. Identification of the von Hippel-Lindau disease tumor suppressor gene. Science 1993;260:1317–20
4. Lamiell JM, Salazar FG, Hsia YE. von Hippel-Lindau disease affecting 43 members of a single kindred. Medicine (Baltimore) 1989;68:1–29
5. Lindau A. Discussion on vascular tumours of the brain and spinal cord. Proc R Soc Med 1931;24:363–70
6. Sabin FR. Preliminary note on the differentiation of angioblasts and the method by which they produce blood-vessels, blood-plasma and red blood-cells as seen in the living chick. J Hematother Stem Cell Res 2002;11:5–7
7. Sabin FR. Studies on the origin of blood-vessels and of red blood-corpuscles as seen in the living blastoderm of chicks during the second day of incubation. Carnegie Contrib Embryol 1920;9:215–62
8. Cushing H, Bailey P. Tumors Arising From the Blood-Vessels of the Brain: Angiomatous Malformations and Hemangioblastomas. Springfield: Charles C. Thomas; 1928
9. Shively SB. *Effects of von Hippel-Lindau (VHL) Gene Deficiency on the Human Central Nervous System*. [PhD Dissertation]. Washington, DC: The George Washington University, Institute for Biomedical Sciences; 2010. ProQuest Direct Complete Database (Publication No. AAT 3426418). Available at: https://www.proquest.com/openview/bd84c87cf828ed1b0da564a60d1be3c7/1?pq-origsite=gscholar&cbl=18750. Accessed January 31, 2011
10. Vortmeyer AO, Gnarra JR, Emmert-Buck MR, et al. von Hippel-Lindau gene deletion detected in the stromal cell component of a cerebellar hemangioblastoma associated with von Hippel-Lindau disease. Hum Pathol 1997;28:540–3
11. Krieg M, Haas R, Brauch H, et al. Up-regulation of hypoxia-inducible factors HIF-1alpha and HIF-2alpha under normoxic conditions in renal carcinoma cells by von Hippel-Lindau tumor suppressor gene loss of function. Oncogene 2000;19:5435–43
12. Flamme I, Krieg M, Plate KH. Up-regulation of vascular endothelial growth factor in stromal cells of hemangioblastomas is correlated with up-regulation of the transcription factor HRF/HIF-2alpha. Am J Pathol 1998;153:25–9
13. Proescholdt MA, Mayer C, Kubitza M, et al. Expression of hypoxia-inducible carbonic anhydrases in brain tumors. Neuro Oncol 2005;7:465–75
14. Wizigmann-Voos S, Breier G, Risau W, et al. Up-regulation of vascular endothelial growth factor and its receptors in von Hippel-Lindau disease-associated and sporadic hemangioblastomas. Cancer Res 1995;55:1358–64
15. Vortmeyer AO, Frank S, Jeong SY, et al. Developmental arrest of angioblastic lineage initiates tumorigenesis in von Hippel-Lindau disease. Cancer Res 2003;63:7051–5
16. Gläsker S, Li J, Xia JB, et al. Hemangioblastomas share protein expression with embryonal hemangioblast progenitor cell. Cancer Res 2006;66:4167–72
17. Huber TL, Kouskoff V, Fehling HJ, et al. Haemangioblast commitment is initiated in the primitive streak of the mouse embryo. Nature 2004;432:625–30
18. Choi K, Kennedy M, Kazarov A, et al. A common precursor for hematopoietic and endothelial cells. Development 1998;125:725–32
19. Zhuang Z, Frerich JM, Huntoon K, et al. Tumor derived vasculogenesis in von Hippel-Lindau disease-associated tumors. Sci Rep 2014;4:4102
20. Gläsker S, Smith J, Raffeld M, et al. VHL-deficient vasculogenesis in hemangioblastoma. Exp Mol Pathol 2014;96:162–7
21. Lonser RR, Glenn GM, Walther M, et al. von Hippel-Lindau disease. Lancet 2003;361:2059–67
22. Shively SB, Beltaifa S, Gehrs B, et al. Protracted haemangioblastic proliferation and differentiation in von Hippel-Lindau disease. J Pathol 2008;216:514–20
23. Vortmeyer AO, Yuan Q, Lee YS, et al. Developmental effects of von Hippel-Lindau gene deficiency. Ann Neurol 2004;55:721–8
24. Vortmeyer A, Tran M, Zeng W, et al. Evolution of VHL tumourigenesis in nerve root tissue. J Pathol 2006;210:374–82
25. Shively SB, Falke EA, Li J, et al. Developmentally arrested structures preceding cerebellar tumors in von Hippel-Lindau disease. Mod Pathol 2011;24:1023–30
26. Maxwell PH. The HIF pathway in cancer. Semin Cell Dev Biol 2005;16:523–30
27. Larsen WJ. Human Embryology. New York: Churchill Livingstone; 1997
28. Sanes DH, Reh TA, Harris WA. Development of the Nervous System. San Diego: Academic Press; 2000
29. Mandriota SJ, Turner KJ, Davies DR, et al. HIF activation identifies early lesions in VHL kidneys: Evidence for site-specific tumor suppressor function in the nephron. Cancer Cell 2002;1:459–68
30. Irizarry RA, Bolstad BM, Collin F, et al. Summaries of Affymetrix GeneChip probe level data. Nucleic Acids Res 2003;31:e15
31. Eisen MB, Spellman PT, Brown PO, et al. Cluster analysis and display of genome-wide expression patterns. Proc Natl Acad Sci USA 1998;95:14863–8
32. Jolliffe IT. Principal Component Analysis. New York: Springer-Verlag; 2002
33. Tukey JW. Exploratory Data Analysis. Reading: Addison-Wesley; 1977
34. Amaratunga D, Cabrera J. Exploration and Analysis of DNA Microarray and Protein Array Data. Hoboken: John Wiley; 2004
35. Cleveland WS. Robust locally weighted regression and smoothing scatterplots. J Am Stat Assoc 1979;74:829–36
36. Lindman HR. Analysis of Variance in Complex Experimental Designs. San Francisco: W.H. Freeman; 1974
37. Benjamini Y, Hochberg Y. Controlling the false discovery rate: A practical and powerful approach to multiple testing. J R Stat Soc Series B Stat Methodol 1995;57:289–300
38. Miller RG. Simultaneous Statistical Inference. New York: Springer-Verlag; 1981
39. Yokota N, Aruga J, Takai S, et al. Predominant expression of human zic in cerebellar granule cell lineage and medulloblastoma. Cancer Res 1996;56:377–83
40. Maricich SM, Herrup K. Pax-2 expression defines a subset of GABAergic interneurons and their precursors in the developing murine cerebellum. J Neurobiol 1999;41:281–94
41. Weisheit G, Gliem M, Endl E, et al. Postnatal development of the murine cerebellar cortex: Formation and early dispersal of basket, stellate and Golgi neurons. Eur J Neurosci 2006;24:466–78
42. Ramón y Cajal S. Sur l'origine et la direction des prolongations nerveuses de la couche moleculaire du cervelet. Internationale Monatsschrift fur Anatomie und. Physiologie 1889;6:158–74
43. Ramón y Cajal S. Histology of the Nervous System of Man and Vertebrates. New York: Oxford University Press; 1995
44. Okuda T, Kokame K, Miyata T. Differential expression patterns of NDRG family proteins in the central nervous system. J Histochem Cytochem 2008;56:175–82
45. Bellamy TC. Interactions between Purkinje neurones and Bergmann glia. Cerebellum 2006;5:116–26

46. Choi BH, Lapham LW. Evolution of Bergmann glia in developing human fetal cerebellum: A Golgi, electron microscopic and immunofluorescent study. Brain Res 1980;190:369–83
47. Yamada K, Watanabe M. Cytodifferentiation of Bergmann glia and its relationship with Purkinje cells. Anat Sci Int 2002;77:94–108
48. Ismail SM, Jasani B, Cole G. Histogenesis of haemangioblastomas: An immunocytochemical and ultrastructural study in a case of von Hippel-Lindau syndrome. J Clin Pathol 1985;38:417–21
49. Böhling T, Mäenpää A, Timonen T, et al. Different expression of adhesion molecules on stromal cells and endothelial cells of capillary hemangioblastoma. Acta Neuropathol 1996;92:461–6
50. Merrill MJ, Sun M, Chen M, et al. The developmental lineage marker PAX2 is expressed in CNS hemangioblastomas in von Hippel-Lindau disease. Neuro-Oncology 2012;14(Suppl 6):vi11–12
51. Cheng L, Arata A, Mizuguchi R, et al. Tlx3 and Tlx1 are post-mitotic selector genes determining glutamatergic over GABAergic cell fates. Nat Neurosci 2004;7:510–7
52. Lv N, Wang Y, Zhao M, et al. The role of PAX2 in neurodevelopment and disease. Neuropsychiatr Dis Treat 2021;17:3559–67
53. Jagannathan J, Lonser RR, Smith R, et al. Surgical management of cerebellar hemangioblastomas in patients with von Hippel-Lindau disease. JNS 2008;108:210–22
54. Kapitsinou PP, Haase VH. The VHL tumor suppressor and HIF: Insights from genetic studies in mice. Cell Death Differ 2008;15:650–9
55. Richards FM, Schofield PN, Fleming S, et al. Expression of the von Hippel-Lindau disease tumour suppressor gene during human embryogenesis. Hum Mol Genet 1996;5:639–44
56. Kanno H, Saljooque F, Yamamoto I, et al. Role of the von Hippel-Lindau tumor suppressor protein during neuronal differentiation. Cancer Res 2000;60:2820–4
57. Murata H, Tajima N, Nagashima Y, et al. Von Hippel-Lindau tumor suppressor protein transforms human neuroblastoma cells into functional neuron-like cells. Cancer Res 2002;62:7004–11
58. Davidowitz EJ, Schoenfeld AR, Burk RD. VHL induces renal cell differentiation and growth arrest through integration of cell-cell and cell-extracellular matrix signaling. Mol Cell Biol 2001;21:865–74
59. Grosfeld A, Stolze IP, Cockman ME, et al. Interaction of hydroxylated collagen IV with the Von Hippel-Lindau tumor suppressor. J Biol Chem 2007;282:13264–9
60. Ji Q, Burk RD. Downregulation of integrins by von Hippel-Lindau (VHL) tumor suppressor protein is independent of VHL-directed hypoxia-inducible factor alpha degradation. Biochem Cell Biol 2008;86:227–34
61. Kurban G, Hudon V, Duplan E, et al. Characterization of a von Hippel Lindau pathway involved in extracellular matrix remodeling, cell invasion, and angiogenesis. Cancer Res 2006;66:1313–9
62. Kurban G, Duplan E, Ramlal N, et al. Collagen matrix assembly is driven by the interaction of von Hippel-Lindau tumor suppressor protein with hydroxylated collagen IV alpha 2. Oncogene 2008;27:1004–12
63. Ohh M, Yauch RL, Lonergan KM, et al. The von Hippel-Lindau tumor suppressor protein is required for proper assembly of an extracellular fibronectin matrix. Mol Cell 1998;1:959–68
64. Russell RC, Ohh M. NEDD8 acts as a 'molecular switch' defining the functional selectivity of VHL. EMBO Rep 2008;9:486–91
65. Luu VD, Boysen G, Struckmann K, et al. Loss of VHL and hypoxia provokes PAX2 up-regulation in clear cell renal cell carcinoma. Clin Cancer Res 2009;15:3297–304
66. Yan B, Jiao S, Zhang H, et al. Prolyl hydroxylase domain protein 3 targets Pax2 for destruction. Biochem Biophys Res Commun 2011;409:315–20
67. Robson EJD, He SJ, Eccles MR. A PANorama of PAX genes in cancer and development. Nat Rev Cancer 2006;6:52–62
68. Tellier AL, Amiel J, Delezoide AL, et al. Expression of the PAX2 gene in human embryos and exclusion in the CHARGE syndrome. Am J Med Genet 2000;93:85–8
69. Dressler GR, Douglass EC. Pax-2 is a DNA-binding protein expressed in embryonic kidney and Wilms tumor. Proc Natl Acad Sci USA 1992;89:1179–83
70. Lawoko-Kerali G, Rivolta MN, Holley M. Expression of the transcription factors GATA3 and Pax2 during development of the mammalian inner ear. J Comp Neurol 2002;442:378–91
71. Zaiko M, Estreicher A, Ritz-Laser B, et al. Pax2 mutant mice display increased number and size of islets of Langerhans but no change in insulin and glucagon content. Eur J Endocrinol 2004;150:389–95
72. Jester R, Znoyko I, Garnovskaya M, et al. Expression of renal cell markers and detection of 3p loss links endolymphatic sac tumor to renal cell carcinoma and warrants careful evaluation to avoid diagnostic pitfalls. Acta Neuropathol Commun 2018;6:107
73. Gläsker S, Lonser RR, Tran MG, et al. Effects of VHL deficiency on endolymphatic duct and sac. Cancer Res 2005;65:10847–53
74. Gläsker S, Tran MG, Shively SB, et al. Epididymal cystadenomas and epithelial tumourlets: Effects of VHL deficiency on the human epididymis. J Pathol 2006;210:32–41
75. Mehta GU, Shively SB, Duong H, et al. Progression of epididymal maldevelopment into hamartoma-like neoplasia in VHL disease. Neoplasia 2008;10:1146–53
76. Liu S, Ginestier C, Charafe-Jauffret E, et al. BRCA1 regulates human mammary stem/progenitor cell fate. Proc Natl Acad Sci USA 2008;105:1680–5